

THE BRITE/EURAM PROGRAMME "HELISHAPE" - A SUCCESSFUL STEP TO BETTER HELICOPTER AERODYNAMIC AND AEROACOUSTIC DESCRIPTION

V. Kloeppe¹, N. Kroll², M. Costes³, L. Morino⁴, I. Simons⁵, W. Splettstoesser⁶, M. Lawson⁷

1 EUROCOPTER DEUTSCHLAND GmbH, München
2, 6 DLR Braunschweig, Germany
3 ONERA Châtillon, France

4 University Roma 3, Italy
5 WHL, Yeovil, Great Britain
7 Bristol University, Great Britain

Abstract

In order to improve performance and public acceptance of current and future helicopters, analytical and experimental investigations on rotor aerodynamics and aeroacoustics have been performed in the research project HELISHAPE funded by the European Community under the BRITE/EURAM programme. Dedicated analytical methods were developed, improved and validated. In addition, helicopter noise reduction measures and quiet helicopter feasibility have been studied. The work was subdivided into six tasks: In the 1st task, two different 3D Euler codes for the description of multibladed hovering rotors have been further developed. In addition, a 2D Navier-Stokes code has been improved to simulate dynamic stall for oscillating airfoils. In task 2, as co-operative activity of several consortium members, a common 3D full potential code has been created for the analytical simulation of the entire helicopter flight regime. In task 3, different existing boundary element methods have been improved in order to describe free wake effects as well as transonic and viscous flows. In task 4, the technical potential of the helicopter to fly neighbourly as well as the feasibility and marketability of such helicopters has been investigated. To evaluate the noise reduction benefits of conceptual blade designs and to generate a data base to validate the aerodynamic / aeroacoustic prediction codes, in task 5, wind tunnel tests with a 4,2 m² model rotor have been performed in the DNW. For the development of efficient rotor noise prediction tools, in task 6, the acoustic analogy method, the Kirchhoff approach and computational aeroacoustics tools have been applied.

Introduction

The objectives of the research programme HELISHAPE, funded by the European Community under the BRITE/EURAM programme, have been to support manufacturers and researchers with deeper knowledge on helicopter aerodynamics and aeroacoustics. Both disciplines are closely connected. The rotor aerodynamics dominates the noise radiation and on the other hand, measures to reduce the acoustic signatures influence heavily the aerodynamic characteristics including the global performance of the helicopter. Therefore, aerodynamic and aeroacoustic research has been combined in an appropriate way. Partners of the project consortium were:

- EUROCOPTER DEUTSCHLAND GmbH - ECD,
- EUROCOPTER FRANCE - ECF,
- AGUSTA SPA,
- GKN WESTLAND HELICOPTER - GKN WHL,

- Deutsche Forschungsanstalt für Luft und Raumfahrt - DLR,
- Office National d'Etudes et de Recherches Aérospatiales - ONERA,
- Centro Italiano Ricerche Aerospaziali - CIRA,
- Defense Research Agency - DRA,
- University of Bristol - U Brist,
- ALFAPI - Institute of Computational Engineering,
- Instituto Superior Technico Lisboa - IST,
- Politecnico di Milano - PMI,
- Technical University of Denmark - TUD,
- Universität Stuttgart - U Stutt.,
- Nationaal Lucht- en Ruimtevaartlaboratorium - NLR

The project comprised 6 tasks which will be described in the following.

Task 1 Euler/Navier-Stokes Equations

Although today, CFD methods are highly developed, the numerical simulation of the flow field around a helicopter rotor still remains a challenging problem. Due to existing limitations in computer resources, physical modelling and numerical algorithms, the development of a general 3D unsteady Navier-Stokes solver for helicopter rotors is not feasible within the near future.

Consequently, within the HELISHAPE project, short term objectives were identified which should lead to useful and improved methods for industry applications.

Prediction of 2D unsteady separated flows

Objective of this subtask was to elaborate the capabilities and merits of unsteady Navier-Stokes solvers for rotor flow related problems by the simulation of 2D unsteady flows around rotor blade sections.

An incompressible, two-dimensional Navier-Stokes code was extended to calculate the turbulent flow around pitching airfoils (Ref. 1.1). The Reynolds stresses are modelled by an eddy-viscosity model which is either determined by the algebraic 0-equation model of Baldwin/Lomax, the 1-equation models of Baldwin/Barth and Spalart/Allmaras or the 2-equation $k-\omega$ models of Wilcox and Menter. Turbulent flows of non-pitching and pitching airfoils were investigated within the project. For the non-pitching case, results for the ONERA-A airfoil at a Reynolds number of 2 million were calculated for low angles of attack, pre-stall and stall conditions. It was found that the various turbulence models examined gave comparable results and in some cases nearly the same result.

Furthermore, calculations for a light stall and a deep stall pitching case were performed. Fig. 1.1 (left) shows that

for the light stall case, the Baldwin/Barth model predicts results in good agreement with measurements. During upstroke, the model agrees very well with the measured values up to about $\alpha=15^\circ$. Also the last part during downstroke is well depicted.

Also for deep stall (Fig. 1.1, right), the considered model results correlate well with measurements. During upstroke, the Baldwin-Barth model compares well with the measurements up to an incidence of about $\alpha=22^\circ$. The model tends to overpredict the peak of the normal force, whereas the one connected to the tangential force is well reproduced. During downstroke, good qualitative agreement with the measurements is obtained, although, large differences are seen locally. In general, the Baldwin-Barth model agrees well with the thrust both during upstroke and downstroke.

Improvement and validation of existing 3D Euler codes for multibladed rotors in hover

The existing Euler codes of DLR and ONERA were improved and extended towards more accurate and efficient prediction methods for multibladed rotors in hover. Since both codes are based on different theoretical approaches, critical components of the solution method were assessed with respect to efficient and accurate unified blade/wake calculations for realistic rotors.

In order to check the reliability of the Euler codes for a wide range of applications, several test cases were selected for common exercise (Ref. 1.2). The computations were performed on common grids allowing a detailed comparison of both codes. For one test case, a grid convergence study was carried out to check the accuracy of the methods. The test cases included the well documented Caradonna-Tung data base as well as the wind tunnel test results of task 5.

Fig. 1.2 shows results for the 4-bladed ECF/ONERA 7AD1 rotor obtained from pre-test computations, which were performed before the corresponding task 5 experiments had been conducted. Predicted and experimental pressure coefficients at five different blade sections are presented. The agreement between experimental and calculated surface data is excellent. Quantitative measurements of the vortex trajectories are compared with predicted values in Fig. 1.3. In conclusion, the pre-test calculations for various tip shapes demonstrate the ability of current Euler methods to perform real predictions of the flow around a realistic rotor in hover. The accurate calculations of surface results indicate that the overall downwash due to the complex wake system is computed correctly without relying on additional wake models. The blind-test calculations demonstrated that no tuning using experimental results is required to predict rotor flows with Euler methods. The ability of an accurate prediction of the tip-vortex position was demonstrated by both Euler methods as long as a separate vortex could be resolved. However, an improved prediction of tip-vortex position and strength will be finally needed in order to predict accurate hovering performance using a Navier-Stokes method.

Task 2 Full Potential Equations

A group of partners jointly developed a Full-Potential CFD method (HELIFP) designed to compute the flowfield around a helicopter rotor blade in hover or forward flight (Ref. 2.1). This activity was a natural follow-on to the previous European BRITE/EURAM project DACRO, where various CFD methods available in Europe to compute helicopter blade flow field were compared to common test cases in order to provide the state-of-the art in this domain in Europe.

The code requirements and specifications were established at the beginning of the project by the industrial partners. They included functionalities, computing speed, memory requirements and standards of coding. During the same period, the industrial partners defined the test cases suitable to validate the code.

These cases cover the full flight envelope of the helicopter (hover, descent flight, high-speed forward flight). Furthermore, some nonlifting forward flight cases were added. A part of the test cases stem from the data base of Task 5.

The second step of the work dealt with the development of the theoretical formulations and algorithms. This work was completed under the responsibility of the Research Establishments and Universities, split into the different items: governing equations, frame of reference, temporal discretisation, spatial discretisation, artificial dissipation, far-field boundary conditions, body boundary conditions, wake boundary conditions, inner section boundary conditions, solver, metrics, grid topology, far wake modelling, etc.

The code characteristics are: conservative full-potential equation written for the fluid at rest, transferred into a frame of reference attached to the blade, fully implicit formulation including boundary conditions with time linearisation and internal Newton iterations, centred finite-volume scheme with lumping to avoid odd-even points decoupling, Enquist-Osher directional flux-biasing to introduce upstream influence in supersonic flows, Riemann invariants applied in the far-field, transpiration condition on the blade able to simulate inflow as well as elastic deformations, implicit transport equation in the wake, 2D perturbation flow for the inboard section, approximate factorisation for pentadiagonal implicit operator, second-order centred spatial differencing to compute the metrics, C-H grid topology (Fig. 2.1), far-wake influence introduced by inflow angle and entropy corrections introduced in order to correct for isentropic flow assumption. The grid generation software was adapted to an already existing algebraic grid generator developed at ONERA.

The third step of the work was devoted to coding. A first version of the code was generated and controlled by quality analysis. Methodological debugging was completed, starting from 2D to 3D, nonlifting to lifting, quasi-steady to unsteady, translational motion to complex rotational motion.

The last part of the project was devoted to the validation of the code by using the test cases defined at the beginning of the project. The results shown describe the chordwise pressure distribution of the 7AD rotor with its

parabolic blade tip tested within task 5. The result for the hovering rotor (Fig. 2.2) is by definition strongly influenced by the inflow model applied - in this case a lifting line model from WHL. In forward flight (Fig. 2.3, blade tip), the solution is less dependent on the inflow model but rather on blade dynamics. Both were computed in this case by the R85/METAR model (Ref. 2.2). Both cases show a fair correlation between theory and test. In particular, the appearance of transonic flow on the blade surface is correctly simulated. Hence, it can be stated that the method is capable to reproduce helicopter rotor flow correctly, although the results are strongly dependent upon a suitable rotor inflow model, which the method cannot provide by itself.

Finally, it should be noted, that here for the first time, a common CFD code was developed by a group of European Partners.

Task 3 Boundary Element Methods

In a first step, two different methodologies and the corresponding computer codes have been developed for the incompressible potential free-wake analysis of helicopter rotors in hover and forward flight under BVI (blade-vortex interaction) conditions. The vortical wakes are determined, at each time step, by convecting in the flowfield the vortical filaments laying on the edges of the blades, the intensity of which has been determined at the previous time step. One approach (Ref. 3.1) is based on a panel-method formulation (whereby the actual geometry of the blade is considered), whereas an alternative one (Ref. 3.2) is based on the lifting surface approach (whereby the blade is modelled as a zero-thickness lifting surface).

Three test cases, taken from the experimental measurements performed in the DNW during the test campaign of the BRITE/EURAM project HELINOISE, have been chosen to assess the ability of the codes in modelling the BVI of rotors. The results obtained have indicated the ability to correctly localise the region of BVI and, for the case of mild BVI effects, to attain a satisfactory, quantitative agreement with the experimental results (Fig. 3.1).

In order to reduce the computational effort without affecting the accuracy of the numerical results, two different simplified wake models have been developed. The first one deals with a wake model for rotors in hover. This consists of a lifting-line formulation with a vortex-lattice wake which includes a semi-infinite far wake model (Ref. 3.3). The near wake is relaxed through a series of successive sweeps, until convergence is reached.

A second approach for rotors in hover and forward flight reproduces the effects of the tip vortex which is approximated by a vortex tube, evaluated via an equivalent disk. Both codes have been successfully validated on the Caradonna and Tung hovering rotor.

In order to cope with the problem of reverse flow in forward flight condition, special treatment for blade sections under reverse flow has been coded to avoid that their 'ill attack flow' causes extreme, unrealistic peaks in wake vorticity. In the extended modelling of Ref. 3.4, the reverse flow blade area is regarded to be

aerodynamically inactive, without any lift and doublet strength activity. As given in Fig. 3.2 for an advance ratio of 0.40, the wake is still shed from the original blade trailing edge, but the doublet strength of both blade and downward shed wake is zero.

In a further step, the applicability of the BEM is extended to non-linear transonic analysis - one of the most advanced applications of BEM to non-linear aerodynamics. Two different boundary integral formulations for the full-potential model are developed and validated. In the first one (formulation A, Ref. 3.5), the differential equation for the potential is written in the form of non-linear Poisson's equation; the linear operator is the Laplacian, and the RHS includes all the compressibility effects (linear and non-linear). A cartesian, non body fitted grid is applied according to Fig. 3.3.

In the formulation B (Ref. 3.6), the full-potential equation has the form of the non-homogeneous wave equation; in this case, the linear operator of the differential equation is the D'Alembert one, and the RHS includes only the non-linear effects.

The main advantage of both formulations is the capability to capture transonic effects (including shock waves) with a field source distribution limited to the region of the flow where the RHSs of the two differential models are not negligible (Fig. 3.3). An example of the Mach number distribution of a typical transonic test case is given in Fig. 3.4.

For method B, a preliminary analysis of the convergence of the method and of its shock capturing capabilities, has been performed for steady two-dimensional problems. The results obtained have been compared to existing Full-Potential and (when applicable) Euler results. So, Fig. 3.5 depicts the pressure coefficient of a NACA 0012 airfoil at $M = 0.82$ with an incidence angle $\alpha = 0^\circ$. Fig. 3.6 presents the c_p distribution of a non-lifting hovering UH-1H rotor at $M_{Tip} = 0.88$. In all the above tests, the algorithm shows interesting shock capturing properties, even with very coarse grids.

The effects of viscosity on the rotor aerodynamics have been addressed by different approaches (Refs. 3.6, 3.7). In particular, a simple shock-boundary layer interaction has been introduced into a boundary integral full-potential code, based on the formulation B (see Ref. 3.6, addressing additionally forward flight, Euler flows and aeroacoustics).

In general, it could be shown that Boundary Element methods represent a very powerful and efficient tool to provide rotor loads and noise sources since they comprise wake generation and require panelling and discretization only in sensitive areas.

Task 4 Quiet Helicopter Feasibility Study

The industry partners assessed the feasibility of producing helicopters significantly less noisy than those available currently. The study has established desirable noise levels, the means by which these targets might be achieved, technological risk areas as well as economic and other penalties. The current status of helicopter flyover noise levels is shown in Fig. 4.1 as a function of

weight along with the CAN 7 and CAN 6 noise limits in Effective Perceived Noise Levels, EPNdB.

Detailed changes to the existing helicopter types can be a first step to generally reduce helicopter noise levels. However, it is likely that a truly quiet helicopter will require a development of more novel configurations (Ref. 4.1). The most direct route towards major noise reductions lies in very low tip speeds. The thrust capability lost hereby can be recovered by large numbers of blades both for main and tail rotors. Encouraging results are predicted for six-bladed rotors with a tip speed of $v_T = 190$ m/s and even more for ten-bladed rotors with a tip speed of $v_T = 160$ m/s (s. Fig. 4.2). The six-bladed rotor offers better payload and performance data than the configuration defined as datum version. It has also the lowest All Up Mass of all variants studied. The design of a ten-bladed main rotor presents major engineering difficulties and is likely to require specific novel solutions to be achievable. Six-bladed rotors exist currently and therefore do not present a significant engineering problem. Lift and/or thrust compounding allows thrust to be recovered at lower tip speeds.

It is important to note that the reduction in rotor noise, brought about by the measures described above will not reduce aircraft overall noise levels by the same amount unless engine noise, in particular, and transmission and airframe noise, to a lesser extent, are reduced commensurately.

Together with design changes, significant improvements can be made by exploiting low noise approach and take off techniques which affect both noise at source and ground contour size. Developments in vehicle control systems and air traffic control techniques will permit the safe and comfortable use of effective noise abatement procedures.

Continued studies into quiet helicopter designs leading ultimately to a full scale technology demonstrator will be necessary before a truly quiet helicopter can be produced. Before a full-scale demonstrator programme is started, certain areas of technology will have to be proved (s. Fig. 4.3). In addition, it will be necessary to establish that any proposed design is acceptable subjectively, i.e. perceived as being quiet. Improved cost models will be required to properly account for the changes in Direct Operating Costs (DOC) and fixed costs of a production aircraft. A programme of engine development will also be required to ensure engine noise is reduced to a satisfactory level and different engine speeds - and hereby blade tip speeds - for varying flight conditions without engine efficiency loss are possible. It is unlikely that funding required for this work package could be recovered by sales of new aircraft alone.

Task 5 Parametric Wind Tunnel Tests

In Task 5, parametric model rotor experiments were successfully conducted in the open-jet anechoic test section of the DNW employing the MWM test rig of DLR/ECD (Ref. 5.1) and a highly instrumented model of a fully articulated ECF/ONERA rotor of 4.2 m diameter, with blades of advanced design and two exchangeable blade tips (Ref. 5.2). One set of blade tips (7A) was of rectangular, the other one (7AD1) of swept-back parabolic

and anhedral shape. The objectives of this experimental research were firstly to provide a high quality data base for validation of the aerodynamic and acoustic codes developed in the other tasks and secondly to evaluate potential noise palliatives. Within the two-weeks wind tunnel entry in 1995, a comprehensive set of simultaneous acoustic and aerodynamic blade surface pressure data as well as blade dynamic and rotor performance data were measured, processed and analysed and made available for the partners. The rotor data were supplemented by selected rotor wake data concerning tip vortex geometry, blade-vortex miss distance, and tip vortex core size (near the tail rotor area) obtained from flow visualization and pressure probe measurements, respectively.

In Figs. 5.1 and 5.2, the test set-up is shown installed in the DNW open test section. Some key results are illustrated in Figs. 5.3 - 5.6. The noise reduction potential of the advanced tip design (7AD1) is demonstrated in Fig. 5.3 for hover at different thrust settings (order of 3 - 4 dBA) and in Fig. 5.4 for high speed level flight with tip speed variation (order of 1 - 4 dBA). This acoustic benefit is the result of the aerodynamically optimized 7AD1 tip design which significantly reduces the supersonic flow region and shock formation on the advancing blade tip (Fig. 5.5) with a beneficial effect also on rotor drag.

Application of the DNW Laser Light Sheet (LLS) flow visualization technique provided quantitative information on tip vortex segments, on the BVI geometry and in particular on the blade-vortex miss distance for typical BVI descent flight conditions (Fig. 5.6) as well as on the wake contraction and vertical wake displacement for hover conditions. In the top view of Fig. 5.6, the Z-axis represents the vertical axis of the wind tunnel, X- and Y-axis define a horizontal plane in which the measured blade position and the measured tip vortex segments are plotted. In the side view (frontal to the blade), the Z-axis represents the shaft axis and the R-axis the blade span. The vertical distance between blade and vortices provides an estimate for the miss distance, the most important parameter for the BVI phenomenon. Extensive analysis of all acquired test data will further physical understanding and accurate prediction of helicopter rotor impulsive noise.

Task 6 Acoustic Codes

This task has grown from work undertaken under the BRITE/EURAM project HELINOISE, and involves a series of linked sub-tasks which concentrate on rotor noise at higher speeds.

The first was a comparison of theory with experiment, using data from HELINOISE and other data available to partners for comparison with theoretical results. This work was expanded during the study to include a round robin examination of the accuracy of acoustic codes from the partners. Excellent agreement between partners was obtained for the fundamental test case, thus confirming the basic accuracy of each partners approach. Some discrepancies were found in more complex test cases (Fig. 6.1) and these are the subject of deeper study. A second part of this work used existing codes from partners, both developed under HELINOISE and elsewhere, to make predictions for comparison with the DNW test data (Fig. 6.2). Since good agreement has

been achieved, the work under this task provided a reasonable basis for future prediction of helicopter noise.

The second set of tasks was associated with the noise from the rotor at high speed. This is one of the major areas of concern in helicopter noise prediction. There are two approaches that have, within current computing resources, the potential for producing accurate predictions of the noise field from a transonic rotor. These are the acoustic analogy formulation, based on the Ffowcs-Williams-Hawkings equation (Ref. 6.1) and the Kirchhoff integral formulation (Refs. 6.2-6.5) which derives the acoustic far field from results based on CFD analysis of the near field close to the rotor (see also Fig. 6.3). Practical implementation of either approach is computationally intensive and demands the introduction of approximations to limit computing requirements. Parallel implementation of both approaches, with comparison for selected test cases to assess the sensitivity of these approximations, has enabled recommendations to be made of the most efficient and accurate approach for noise prediction under various operating conditions.

The results from these studies have been highly instructive. For speeds below delocalisation, good accuracy can be achieved by using the Lighthill acoustic analogy approach in its various forms. A useful increase in accuracy for the higher speed part of this regime can be achieved by including additional quadrupole terms in the formulation. However, at the highest forward speeds where the rotor is surrounded by a shock field which streams away from the rotor (delocalisation), accurate computation of the quadrupole field requires carefully constructed volume integration processes which are exactly parallel to those required in conventional Euler code approaches. This is unsurprising since the key singularity issues arise directly from the details of the shock geometry. Thus the issues in the quadrupole models were found to have features in common with those of the CFD kernel of the Kirchhoff based approach to sound prediction. In the intermediate regime, it was demonstrated that both approaches gave equivalent results (see Fig. 6.4).

The third task was centred on Computational Aeroacoustics, CAA (Refs. 6.4, 6.5). This approach is based on conventional CFD but in principle is directed more specifically at aeroacoustic problems. Results show that it is not possible to obtain reliable acoustic pressure data more than a few chords away from the aerofoil on grids that can fit into current computer memories. A fundamental study of the capability of the upwind scheme to propagate an acoustic disturbance has demonstrated that typically 40-80 grid points per wavelength are required if the pressure amplitude is to be properly resolved. The conclusions of the study is that the only feasible (and accurate) method is to use the computational method to provide near-field pressure data for use with a Kirchhoff surface method for predicting the far-field acoustic pressures.

These conclusions have been confirmed by independent studies at two partners using significantly different flow algorithms and gridding approaches. Direct comparison of codes from two partners using very different

approaches to the unsteady codes was also made. This comparison proved very informative for both partners, and after some iteration mutual agreement of the results was obtained. In particular, it was found possible to follow shocks leaving the aerofoil during their propagation. Methods were also developed which could accurately represent the tip region even for complex geometries at high speed.

Some work was also undertaken on the further development of broad band models for helicopter noise (Ref. 6.6). A final part of the work was the development of a common European computational shell within which the codes developed during the present work, and elsewhere, could be implemented.

Conclusions

The partners of the project HELISHAPE have been successful in setting up the aerodynamic / aeroacoustic basis for the design of modern helicopters and for the improvement of existing ones. In detail, the following results have been attained:

In the case of Navier-Stokes analysis, the 2D stall computations with the eddy-viscosity model of Baldwin/Barth describe blade loading in good agreement with tests.

Current Euler methods have been proven to perform real predictions of the flow around a realistic rotor in hover without relying on additional wake models. The ability of an accurate prediction of the tip-vortex position was demonstrated as long as a separate vortex could be resolved. However, an improved prediction of tip-vortex position and strength will be finally needed in order to predict accurate hovering performance using a Navier-Stokes method.

A Full Potential code was commonly developed capable to reproduce helicopter rotor flow correctly. In particular, the appearance of transonic flow on the blade surface could be shown to be correctly simulated. Since the method is not capturing the rotor wake it has to be coupled with a suitable rotor inflow model.

It could be shown that Boundary Element methods represent a very powerful and efficient tool to provide rotor loads and noise sources since they comprise wake generation and require panelling and spatial discretization only in sensitive areas - for transonic flows, only the volume around the blade tip. For the hover case, capturing of transonic effects including shocks could be proven.

In the area of aeroacoustics, at lower speeds very good agreement between direct Euler computations and analysis using the Euler results in combination with acoustic analogy approaches could be obtained. For high-speed cases above delocalisation, a full CFD computation is required. Thus, providing that the Kirchhoff box is positioned outside the regime in which non-linear effects are significant, accurate predictions of the pressure disturbance at farfield microphone locations can be obtained with flowfield computations confined to the nearfield. In contrast, application of the CFD/Kirchhoff method for computations at lower speeds where non-linear effects are insignificant, requires fine meshes and a

high computational effort, so that the acoustic analogy approaches will be considerably more effective.

The wind tunnel test results attained in the DNW serve to validate the partners' aerodynamic / aeroacoustic codes and to choose appropriate rotor blade tip speeds complying with both performance and noise reduction requests.

The Quiet Helicopter Study serves as manufacturers' orientation towards new low noise designs by providing both future market and certification scenarios and an assessment of the available noise reduction means.

Continued studies into quiet helicopter designs leading ultimately to a full scale technology demonstrator will be necessary before a truly quiet helicopter can be produced.

Work on relevant aspects of CFD development and wind tunnel testing is continued in the current BRITE/EURAM projects EROS (Euler method for rotors), HELIFUSE (Navier-Stokes code for fuselages) and HELIFLOW (wind tunnel test technology for interaction phenomena).

References at the end of the paper

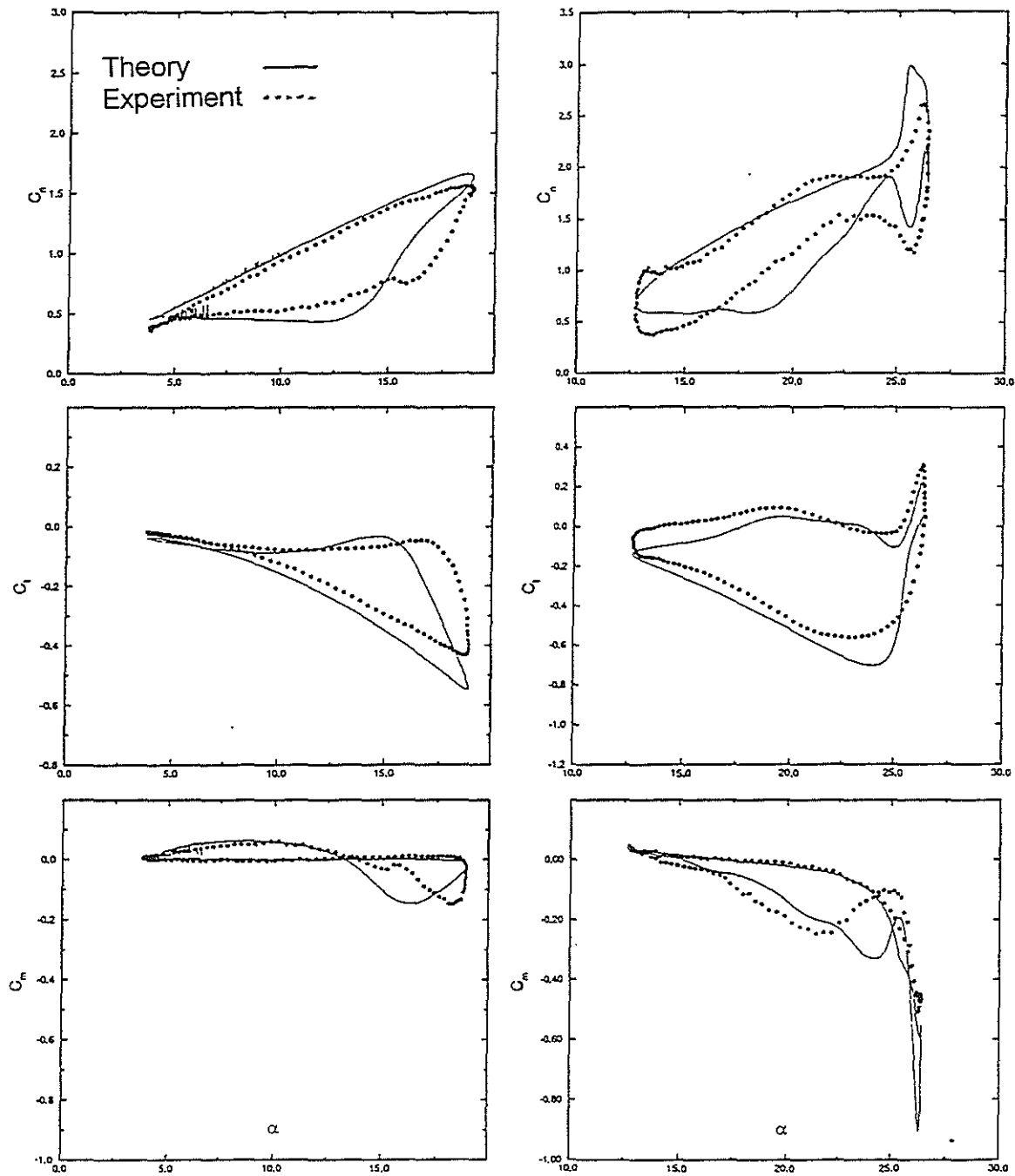


Fig. 1.1 C_n , C_t , C_m of NACA 0015 airfoil, turbulence model: Baldwin/Barth. Left: light stall ($k=0.102$, $\bar{\alpha} = 11,37^\circ$, $\Delta\alpha = 7,5^\circ$), Right: deep stall ($k=0,154$, $\bar{\alpha} = 19,58^\circ$, $\Delta\alpha = 6,83^\circ$),

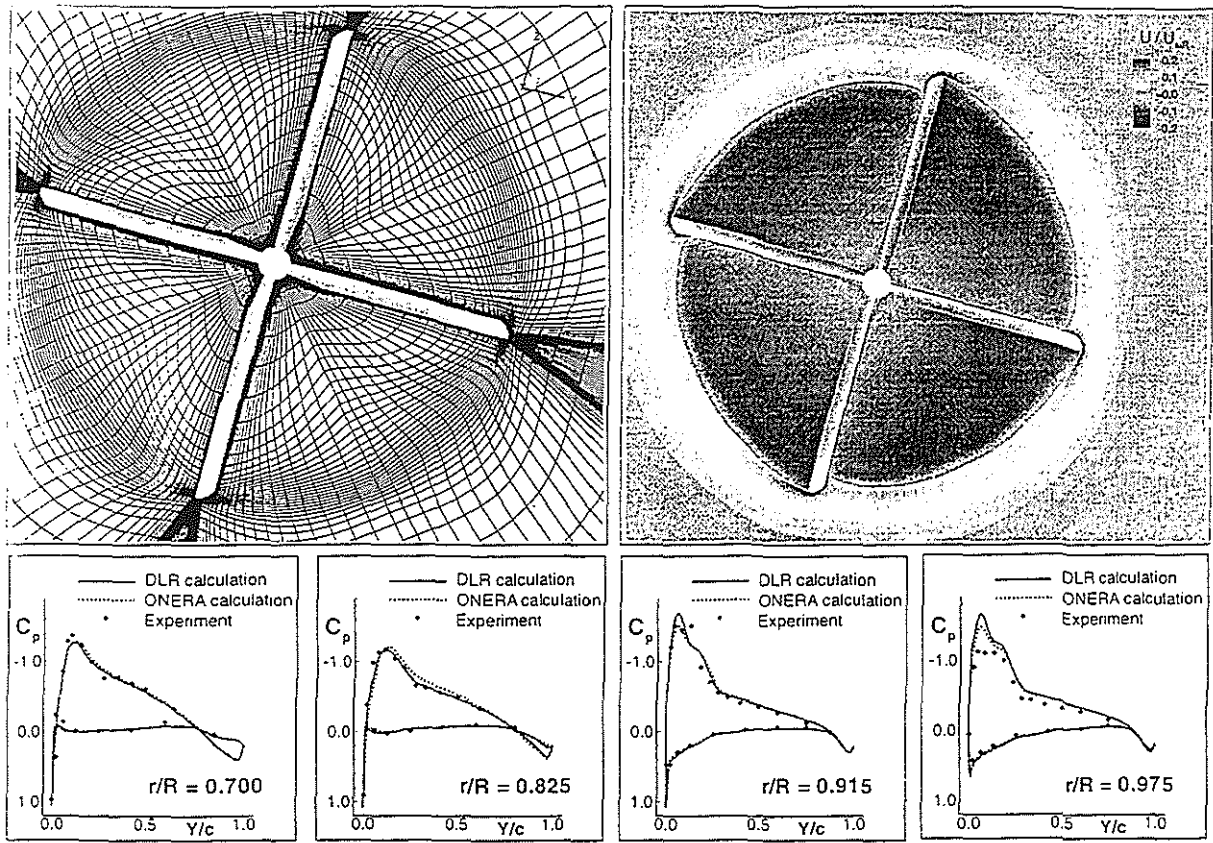


Fig. 1.2 Comparison of surface pressure distribution for the HELISHAPE 7A-D1 rotor

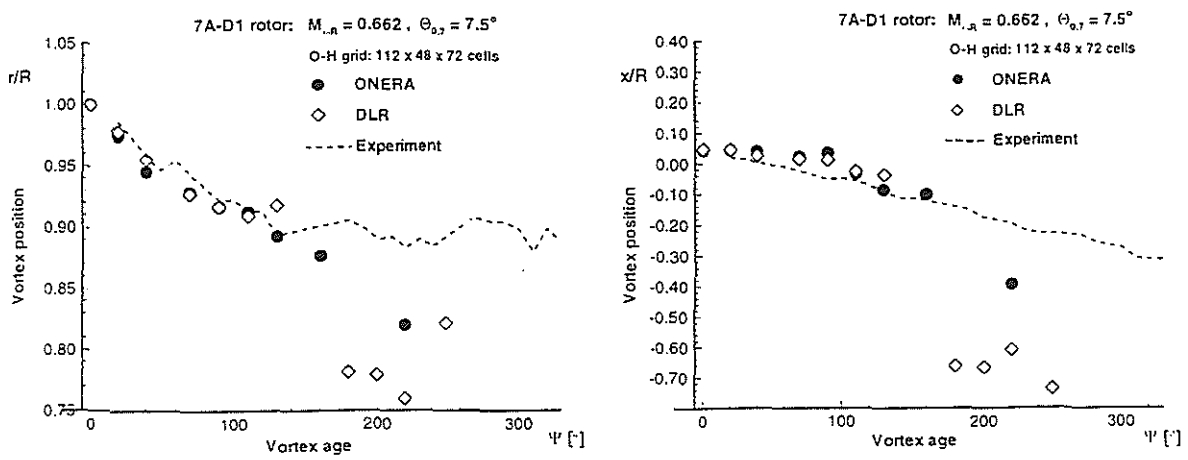


Fig. 1.3 Comparison of vortex trajectories for HELISHAPE 7A-D1 rotor

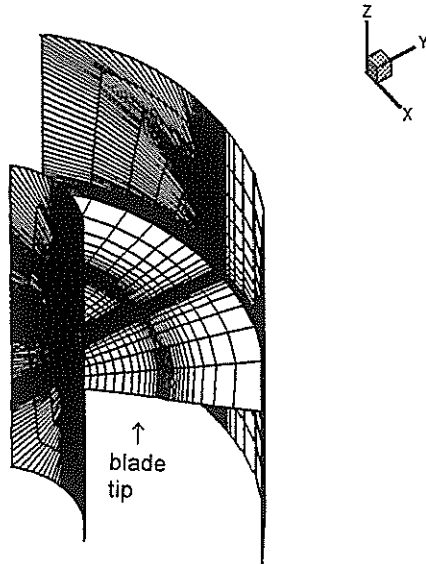


Fig. 2.1 Grid set up for the Full Potential computations.

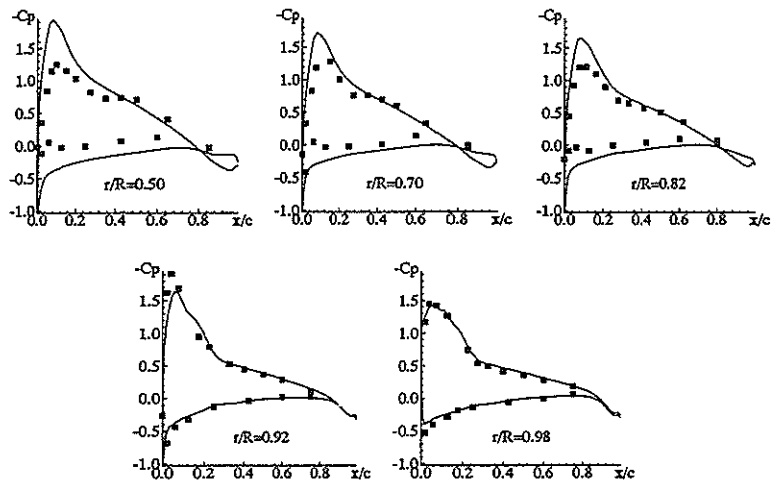


Fig. 2.2 C_p distribution of 7AD model rotor in hover. Test results (*) from HELISHAPE

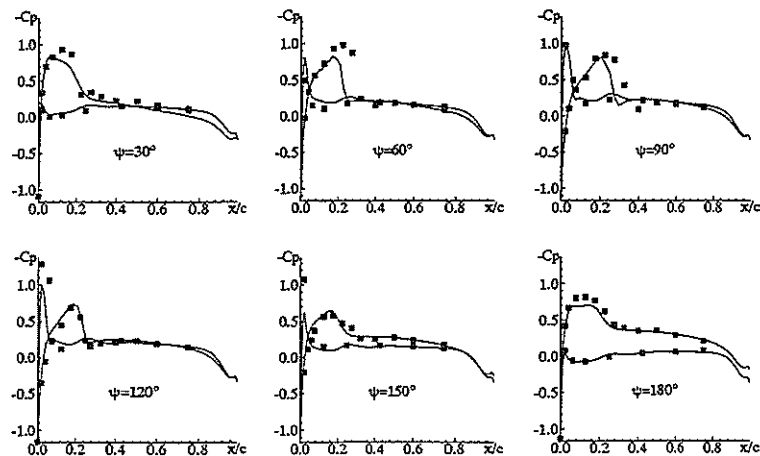


Fig. 2.3 C_p distribution of the 7AD model rotor in forward flight at $r/R=0,975$ for different azimuth positions, $M_{\omega R}=0,616$, $\mu=0,355$. Test results (*) from HELISHAPE tests

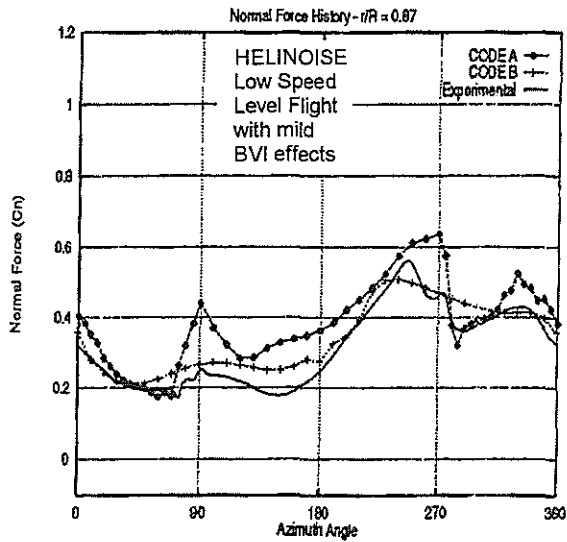


Fig. 3.1 C_N distribution computed by panel methods with finite blade thickness (code A) and zero thickness (code B), $\mu=0,151$, $c_T=0,00446$

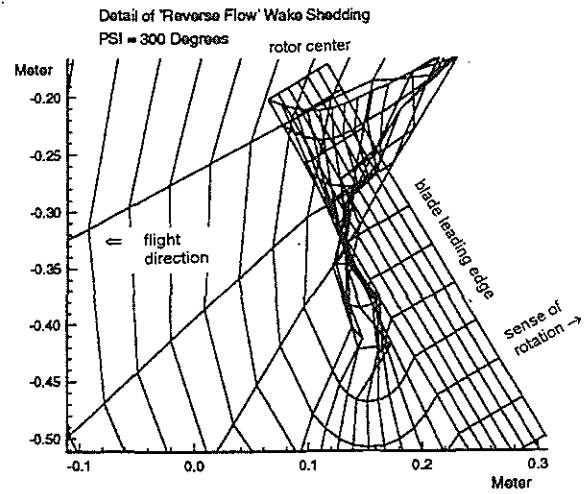


Fig. 3.2 Rotor wake at fast forward flight, strong reverse flow

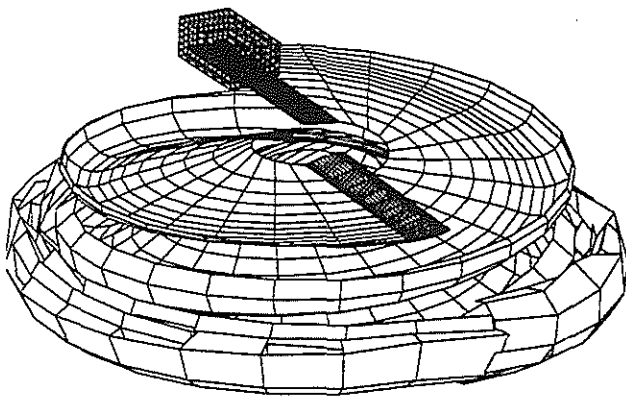


Fig. 3.3 Volume discretization in transonic zone (Method A)

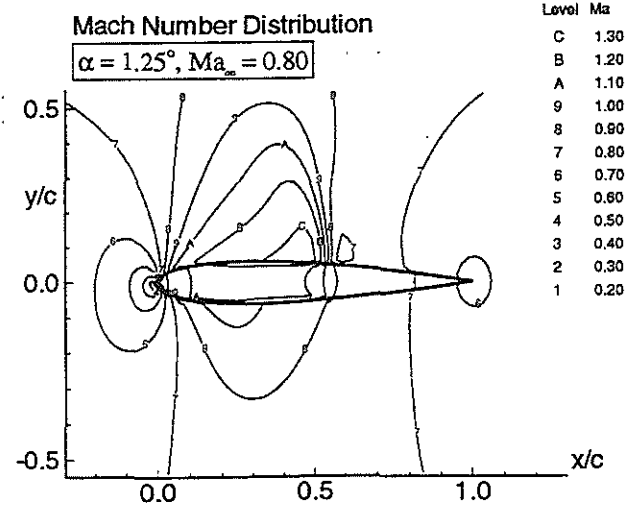


Fig. 3.4 Distribution of Mach number evaluated by method A in the transonic region at the blade tip of a hovering rotor

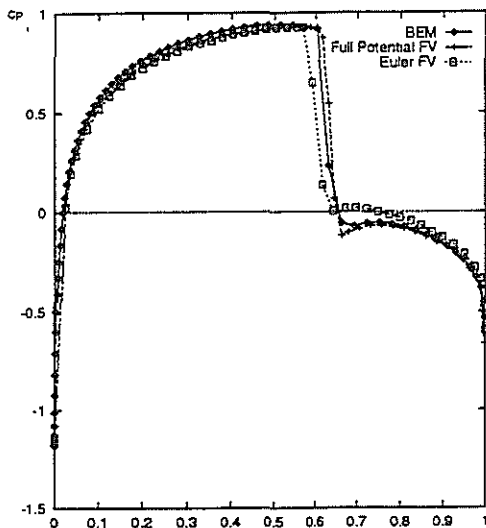


Fig. 3.5 C_p distribution of a NACA0012 airfoil at $M=0,82$ with incidence angle $\alpha=0^\circ$

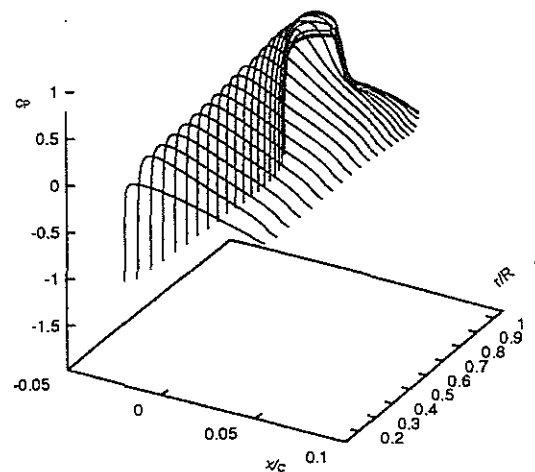


Fig. 3.6 C_p distribution of a non-lifting hovering UH-1H rotor at $M_{Tip}=0,88$

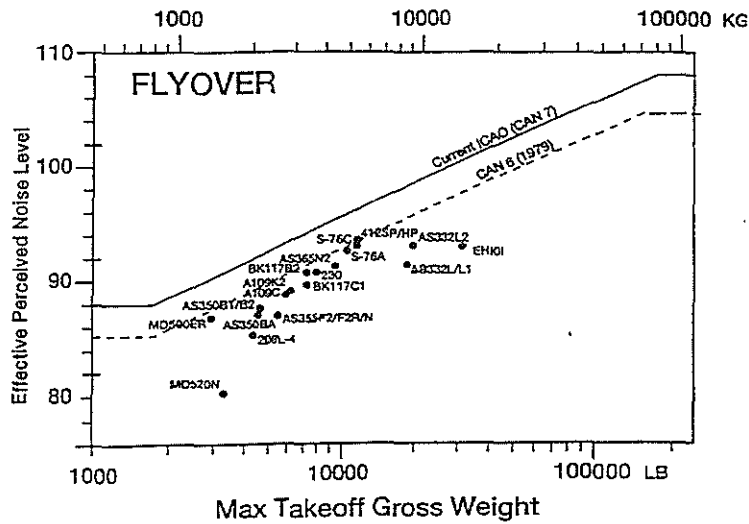


Fig. 4.1
ICAO certification limits - Flyover

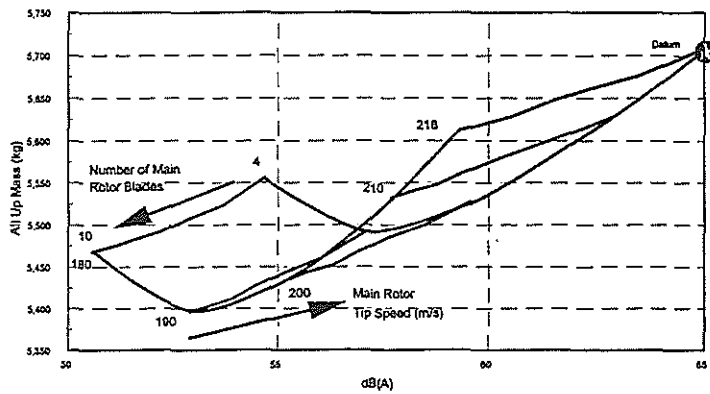


Fig. 4.2
Influence of number of main rotor blades and tip speed on All Up Mass and A-weighted noise level
Diameter: 13,5 m
Solidity: 10,5%

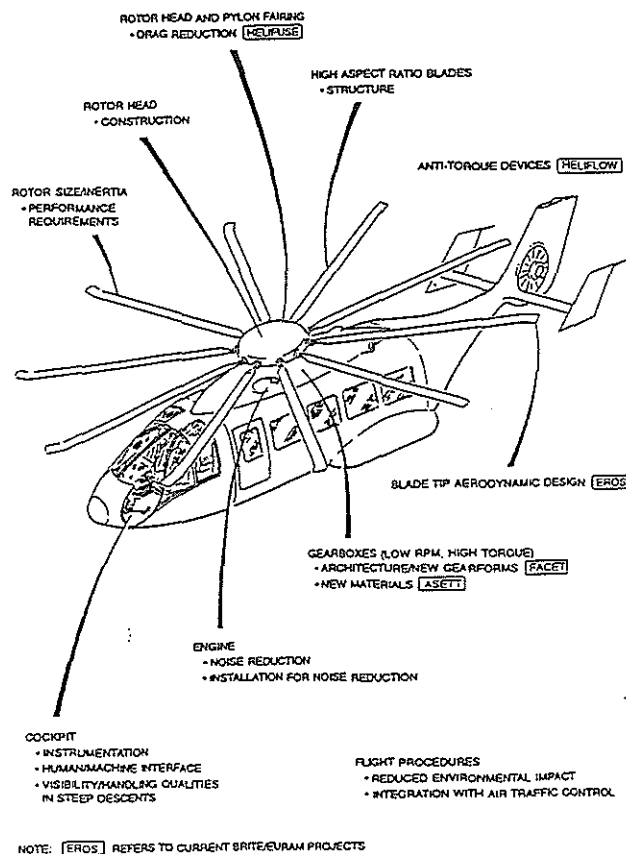


Fig. 4.3
Current and Future Quiet Helicopter research areas

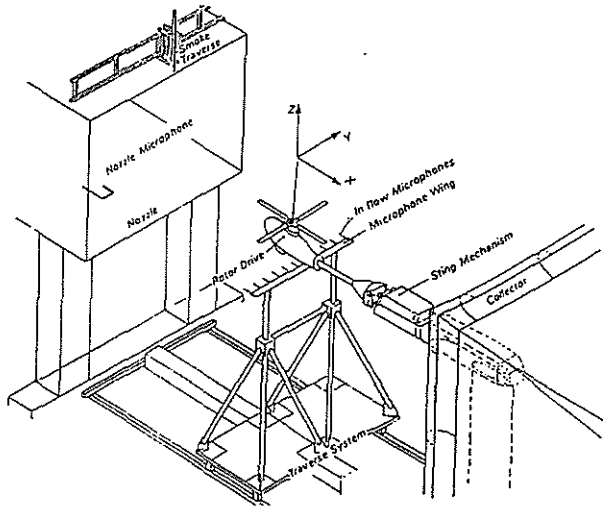


Fig. 5.1 DNW test set-up for aeroacoustic tests

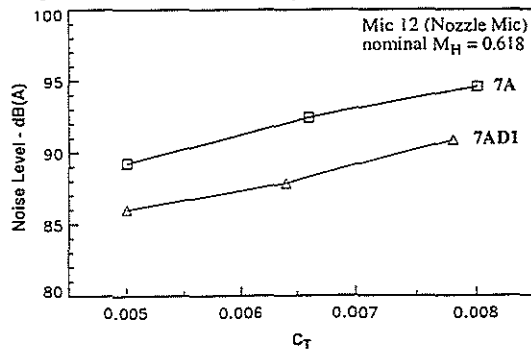


Fig. 5.3 In-plane measured A-weighted levels for 7A and 7AD1 rotor vs hover thrust

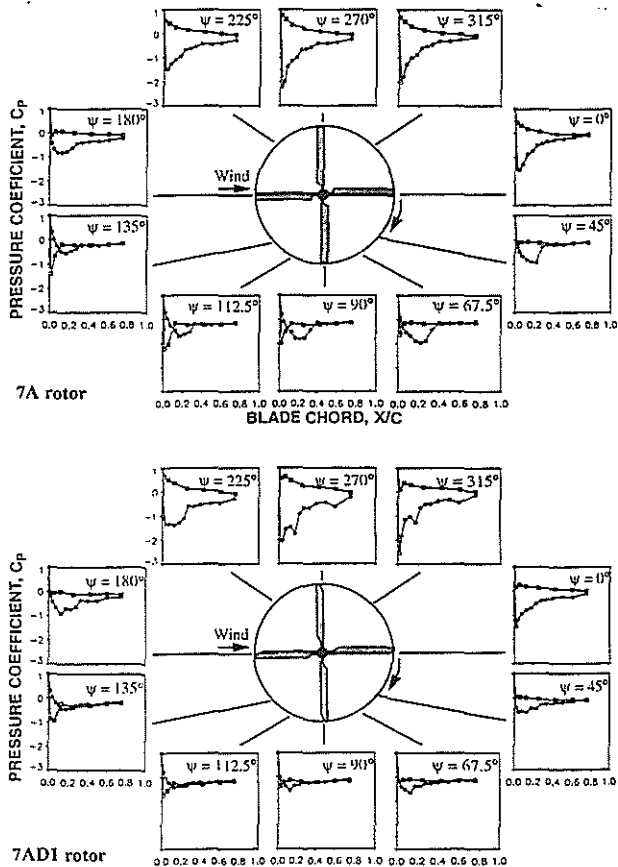


Fig. 5.5 Chordwise blade pressure distribution for 7A and 7AD1 rotor vs blade azimuth for $v=76$ m/s, $r/R=0,975$

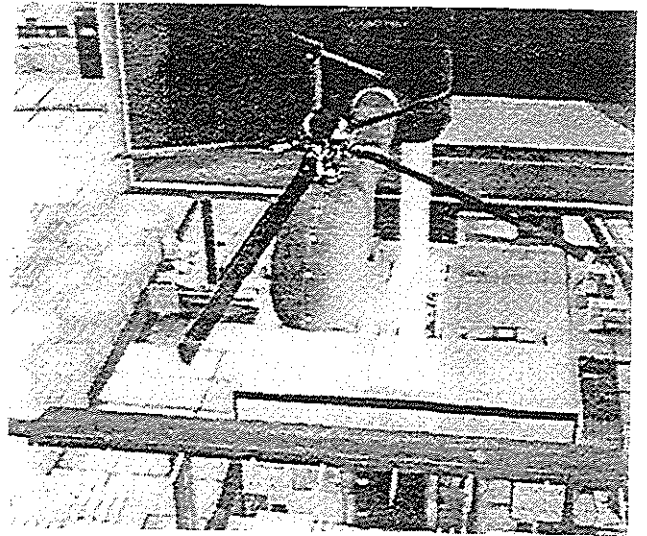


Fig. 5.2 7AD1 model rotor in the open DNW test section and moveable microphone array

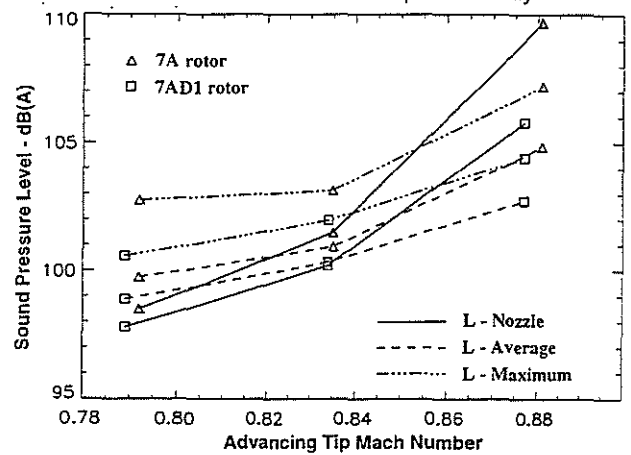
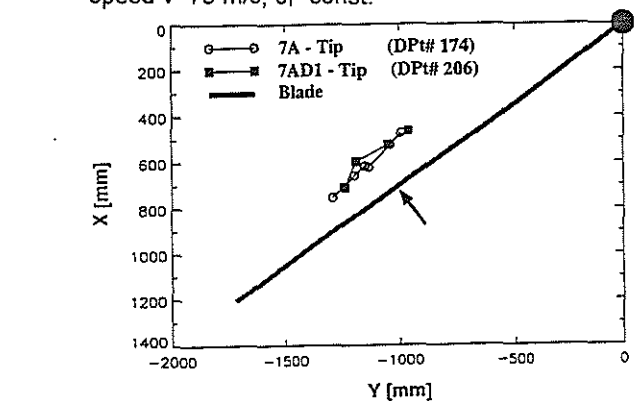


Fig. 5.4 7A and 7AD1 in-plane A-weighted sound levels vs tip Mach number at level flight speed $v=76$ m/s, $C_T=const.$



$V_\infty = 35$ m/s
 $\alpha_{shaft} = 5,7^\circ$
 $\mu = 0,167$
 $C_T = 0,0069$

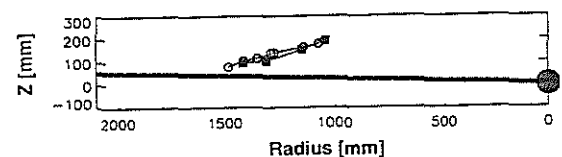


Fig. 5.6 Vortex trajectories determined by LLS-technique at 55° blade azimuth for a 6° descent flight condition

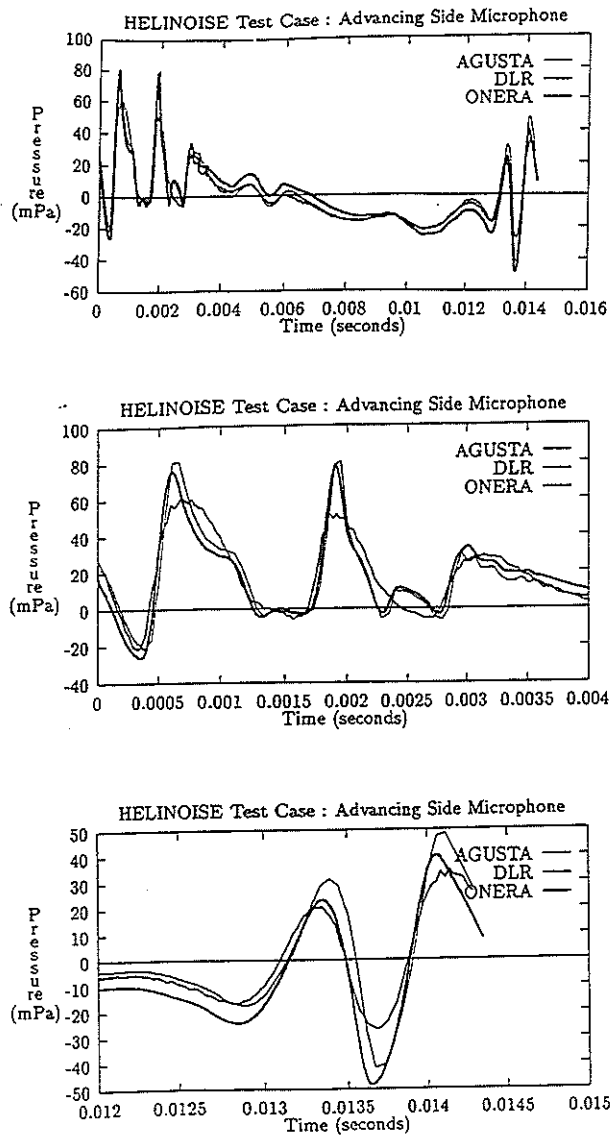
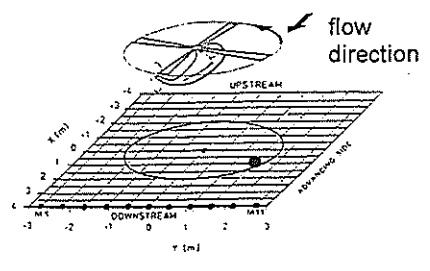


Fig. 6.1 Comparison of partners' codes



sound pressure time history at ●

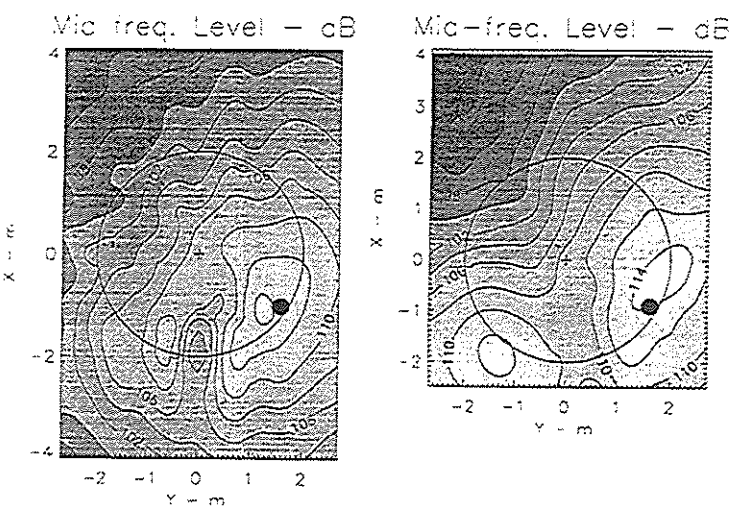
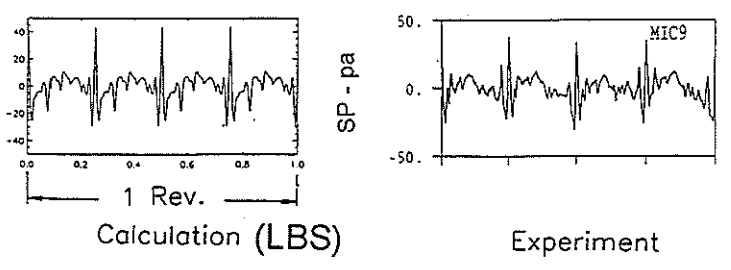


Fig. 6.2 HELINOISE test results vs FWH analysis, blade pressures produced by a Lifting Body Surface method

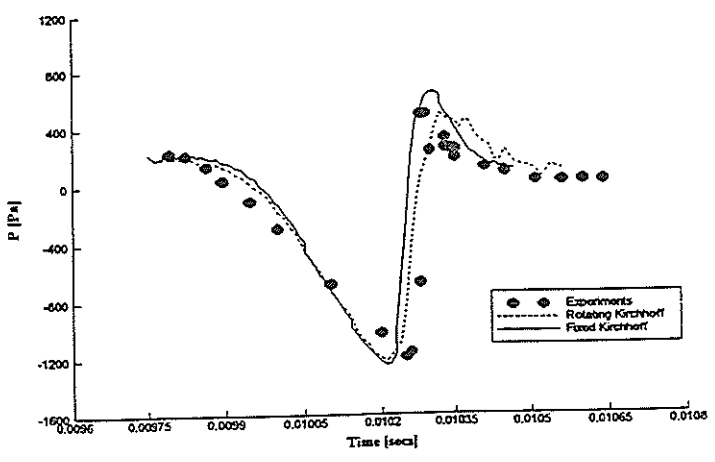


Fig. 6.3 Comparison of Kirchhoff solutions with experimental data

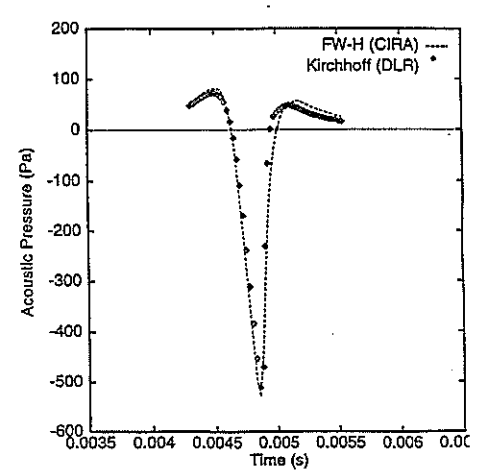


Fig. 6.4 Comparison between FWH and Kirchhoff results

References

- 1.1 Soerenesen, J.N., Michelsen, J.A., Hansen, M.O.L., Nygreen, P.J., Sorensen, D.N., "Incompressible Navier-Stokes Models for Aerodynamic Flows", in "Advances in Fluid Mechanics", Vol. 11, pp 185-224
- 1.2 Rouzaud, O., Boniface, J.Ch., Raddatz, J. "Euler Calculations of Multibladed Rotors in Hover by DLR and ONERA Methods and Comparisons with HELISHAPE Tests", 53rd Forum of AHS, Virginia Beach 1997
- 2.1 Costes, M., Le Balleur, J.C., Gasparini, L., Vigevano, L., Hounjet, M.H.L., Kokkalis, A., Miller, J.V., Spruce, M., Pagano, A., Renzoni, P., Rocchetto, A., Toulmay, F., "Development of a Common European Unsteady Full Potential CFD Code for Rotors in Hover and Forward Flight", 53rd Forum of AHS, Virginia Beach, 1997
- 2.2 Arnaud, G., Beaumier, P., "Validation of R85/METAR on the Puma RAE Flight Tests", 18th ERF, Avignon, 1992
- 3.1 Visingardi, A., D'Alascio, A., Pagano, A., Renzoni, R. "Validation of CIRA's Rotorcraft Aerodynamic Modelling System with DNW Experimental Data", 22nd ERF, Brighton, 1996
- 3.2 Baron, A., Boffadossi, M., DePonte, S., "Numerical Simulation of Vortex Flows Past Impulsively Started Wings", in AGARD-CP-494, "Vortex Flow Aerodynamics", 1990
- 3.3 Brown, K.D., Fiddes, S.P., "New Developments in Rotor Wake Methodology", 22nd ERF Brighton, 1996
- 3.4 Zerle, L., Wagner, S. "Influence of Inboard Shedded Rotor Blade Wake to the Rotor Flow Field", 19th ERF, Como 1993
- 3.5 Röttgermann, A. "Eine Methode zur Berücksichtigung kompressibler und transsonischer Effekte in Randelementenverfahren", Doctoral Thesis Universität Stuttgart, Institut für Aerodynamik und Gasdynamik, 1995
- 3.6 Gennaretti, M., Iemma, U., Salvatore, F., Morino, L., "Recent Developments on a BEM for Aerodynamics and Aeroacoustics for Rotors", 23rd ERF, Dresden, 1997
- 3.7 Papanikas, D.G., Spyropoulos, A.J., Fertis, D.K., Margaris, D.P., "Helicopter Downwash Calculation Using the Vortex Element Method for the Wake Modelling", 20th International Conference in Aeronautics, Sorrento, 1996, Paper ICAS-96-2.4.3
- 4.1 Leverton, J.W., "The Potential for Quiet Rotorcraft", 16th AIAA Aeroacoustics Conference, Munich, 1995
- 5.1 Stephan, M., Klöppel, V., Langer, H.-J., "A New Wind Tunnel Test Rig for Helicopter Testing", 14th ERF, 1988
- 5.2 Schultz, K.J., Spletstoesser, W., Junker, B., Wagner, W., Schoell, E., Arnaud, G., Mercker, E., Pengel, K., Fertis, D., "A Parametric Wind Tunnel Test on Rotorcraft Aerodynamics and Aeroacoustics (HELISHAPE) - Test Procedures and Representative Results", 22nd ERF, Brighton 1995
- 6.1 Ianniello, S., deBernardis, E., "Volume Integration in the Calculation of Quadrupole Noise from Helicopter Rotors", 16th AIAA Aeroacoustics Conference, Munich, 1995
- 6.2 di Francescantonio, P., "A Supersonically Moving Kirchoff Surface Method for Delocalized High Speed Rotor Noise Prediction", 2nd AIAA/CEAS Aeroacoustics Conference, State College, PA, 1996.
- 6.3 Polacsek, C., Costes, M., "Rotor Aeroacoustics at High Speed Forward Flight Using a Coupled Full Potential/Kirchoff Method", 21st ERF, St. Petersburg, 1995
- 6.4 Kuntz, M., "Rotor Noise Predictions in Hover and Forward Flight Using Different Aeroacoustic Methods", 2nd AIAA/CEAS Aeroacoustics Conference, State College, PA, 1996
- 6.5 Mundt, R., "The Prediction of the Acoustic Radiation from a Hovering Rotor Blade Using the Kirchoff Method and Description of Associated KIRAC Code", DERA Report number DERA/ASD/CR97020/1, 1997
- 6.6 Campos, L.M.B.C., Macedo, C.M., "On the Prediction of the Broadband Noise of a Helicopter Rotor from the Impulsive Component", Journal d'Acoustique 5, pp. 531-542, 1992